Investigation of the conformational flexibility of DGAT1 peptides using tryptophan fluorescence

2015 Methods Appl. Fluoresc. 3 025003

(http://iopscience.iop.org/2050-6120/3/2/025003)

Methods and Applications in Fluorescence

RECEIVED
6 November 2014

REVISED
16 January 2015

ACCEPTED FOR PUBLICATION
26 January 2015

PUBLISHED
27 March 2015

PAPER

Investigation of the conformational flexibility of DGAT1 peptides using tryptophan fluorescence

Jose L S Lopes[1,2], Ana P U Araujo[1] and David M Jameson[2]

[1] Institute of Physics of Sao Carlos, University of Sao Paulo, Sao Carlos, SP, Brazil
[2] Department of Cell and Molecular Biology, University of Hawaii at Manoa, Honolulu, HI, USA

E-mail: djameson@hawaii.edu

Keywords: diacylglycerol acyltranferase, fluorescence spectroscopy, peptide-lipid interaction, phasor plots, time-resolved fluorescence

Abstract

The conformational behavior of synthetic peptides corresponding to the putative binding sites of the diacylglycerol acyltransferase 1 enzyme (a polytopic integral membrane protein) was investigated using steady-state and time-resolved fluorescence spectroscopies. Three small linear peptides with 13, 15 and 22 amino acid residues, containing one, two and three Trp residues, respectively, were studied in aqueous solution, in the absence and presence of model membranes. The high flexibility and unordered conformation of the peptides in solution were confirmed by the low Trp polarization values, the high accessibility to water-soluble quencher, and the fast rotational correlation times of the Trp residues. However, upon binding to the lipid systems, the Trp residues were incorporated within the acyl hydrophobic core and their lifetimes and rotational correlation times increased. Phasor plots were employed to analyze intensity decay of peptide-lipid binding and provided a trajectory, in phasor space, that lies along a line connecting the points of the free and bound peptide. This trajectory was analyzed to determine the association constant of the peptide to the model membrane.

S Online supplementary data available from stacks.iop.org/MAF/3/025003

1. Introduction

Diacylglycerol acyltransferase 1 (DGAT1) is a polytopic integral membrane protein [1–3] found in the endoplasmic reticulum (ER) phospholipid bilayer, where this enzyme is recruited for the synthesis of triglycerides in many organisms. Although DGAT1 is seen as an important potential therapeutic target for treating obesity-related diseases [4] and other metabolic disorders in humans [5–7], due to its very hydrophobic nature, there is little structural information, i.e. no crystal structure is available for it or any close homolog enzyme.

Recent studies with the bovine DGAT1 have used bioinformatics approaches to identify regions of this protein that are identical to portions of other enzymes acting on the same substrates (acyl-CoAs and diacylglycerols) [8], which include a conserved motif between the DGAT1 and acylcholesterolacyltransferase (ACAT) and a potential substrate binding site which supposedly interact with diacylglycerols. Moreover, biophysical methods have been used to investigate the interaction of the putative binding sites of the bovine DGAT1 with substrates for the triglyceride synthesis and model membranes [8]. Since the corresponding regions of the peptides must play an important role in substrate recognition and binding, an understanding of the driving forces that promote the folding and/or conformational changes in these regions of the enzyme can contribute to a clearer understanding of how the activity of DGAT1 is controlled. Given that DGAT1 represents an interesting target for metabolic diseases, it is important that its structure-activity relationships are fully characterized.

Fluorescence spectroscopy methods are widely employed for investigations of molecular processes, such as protein conformation and dynamics [9]. Studies utilizing intrinsic protein fluorescence are usually based on investigations of excitation/emission spectra, quantum yields, polarizations/anisotropies and excited state lifetimes of the amino acid tryptophan (Trp), the aromatic residue that usually dominates protein fluorescence and which is used as a sensitive probe to study the conformational dynamic of its microenvironment. In the present study, both steady-state and time-resolved fluorescence methodologies were used to investigate the structural flexibility of the synthetic peptides of the DGAT1 enzyme and to analyze their conformational

behavior upon interaction with model membranes. These biophysical approaches provide useful insights into the interaction of DGAT1 with biomembranes and its access to substrates.

2. Experimental section

2.1. Synthetic peptides and model membranes

The three small peptides, named Sit1 (^{356}FGDREFYRDWWNSES^{370}), Sit2 (^{379}NIPVHKWSIRHFY^{391}) and Sit1 and 2 (^{356}FYRDWWNSESGSGHKWSIRHFY^{391}) were synthesized as described in Lopes *et al* [8]. Peptide concentration was determined by measuring the absorbance at 280 nm, using molar extinction coefficients of 12 490, 6 990 and 19 480 $M^{-1}cm^{-1}$ for Sit1, Sit2 and Sit1 and 2, respectively.

Surfactant stock solution of sodium dodecyl sulfate (SDS), N-hexadecyl-N, N-dimethyl-3-ammonio-1-propanesulfonate (HPS) or cetyltrimethylammonium bromide (CTABr) were prepared in 10 mM sodium phosphate (PBS, pH 7.2). All surfactants were purchased from Sigma-Aldrich (St Louis, MO).

2 2. Intrinsic tryptophan emission spectra

The steady-state emission spectrum of each peptide (7 μM) in PBS (pH 7.2) and/or in the presence of detergents (10 mM) was measured on an ISS PC1 spectrofluorimeter (ISS Inc., Champaign, IL) with excitation performed at 300 nm, using 8 nm slits for both excitation and emission and 1 cm pathlength quartz cuvettes (Hellma USA Inc., Plainview, NY). Emission spectra, viewed through a parallel polarizer, were recorded from 310 to 450 nm in 1 nm intervals, at 25 °C, with the temperature controlled via a circulating water bath (Fisher Scientific, Pittsburgh, PA). Final emission spectra were corrected for the wavelength-dependent response of the emission optics [9].

2.3. Fluorescence polarization studies

The excitation polarization spectra of the DGAT1 peptides in aqueous solution (PBS, pH 7.2) and in the presence of 50% glycerol (Fisher Sci.) at 25 °C, and in 100% glycerol at 5 °C, using a 0.3 cm pathlength quartz cuvette (Hellma) were collected on an ISS PC1 spectrofluorimeter (ISS Inc., Champaign, IL), using calcite polarizers. Emissions at wavelengths longer than 338 nm were viewed through longpass filters. Excitations were performed over the wavelength range from 260 to 310 nm. Fluorescence polarization (P) was determined as a function of the parallel ($I_{\|}$) and the perpendicular ($I_{\perp}$) fluorescence intensities, according to the equation: [9]

$$P = \frac{I_{\|} - I_{\perp}}{I_{\|} + I_{\perp}} \quad (1)$$

2 4. Determination of quantum yield

The relative quantum yield of each peptide was determined using L-Trp (Sigma-Aldrich) as a standard ($\Phi = 0.14$) [10]. Measurements were performed with the samples in PBS (pH 7.2) or in the presence of micelles by adjusting the optical density of each peptide and the standard to <0.05 at 300 nm, using 1 cm pathlength quartz cuvettes, with 300 nm excitation with vertical polarized light, and 8 nm slits. Emission spectra were collected from 310 to 450 nm in triplicate, using 8 nm slits, with the polarizers at magic angle conditions (parallel excitation and 55° emission). Alternatively, total fluorescence intensity ($I_{\|} + 2I_{\perp}$) was also collected for each sample, using parallel polarized excitation.

2.5. Fluorescence quenching assays

The degree of exposure of the Trp residues of the DGAT1 peptides to the aqueous environment upon lipid binding was monitored by acrylamide quenching assays. Aliquots (2.5 μL) of an acrylamide stock solution (8 M) were titrated into a cuvette containing 2 mL of each peptide (1 μM) in the range from 0 to 0.1 M. Excitation was set at 295 nm and emission spectra were recorded from 305 to 450 nm in duplicate, in the absence or in the presence of the micelles (10 mM), through WG320 nm emission filters (to minimize Raman contributions), using 8 nm slits, at 25 °C. The Stern–Volmer quenching constants (K_{sv}) were obtained from the slope of the curves using the equation: [9]

$$\frac{F_0}{F} = 1 + K_{SV}[Q] \quad (2)$$

where F_0 and F are the fluorescence intensities in the absence and in the presence of quencher (Q), respectively and K_{SV} is the Stern–Volmer quenching constant. The observed intensities were corrected for dilution.

2.6. Fluorescence titration assays

The binding of the Sit1 peptide to the micelles was measured on an ISS PC1 spectrofluorimeter (ISS Inc., Champaign, IL) with excitation performed at 280 nm with a 280 nm interference filter (Semrock Inc., Rochester, NY) in the excitation path, using 2 mm slits, and a 1 cm pathlength quartz cuvette, at 25 °C. Initially, the free peptide Sit1 (0.5 μM) in PBS was titrated into the formed micelles of HPS and CTAB (13 mM), and the corresponding emission spectra were recorded from 310 to 450 nm, in 1 nm intervals, through 330 nm longpass filters. Polarizations and total fluorescence intensities were monitored at wavelengths longer than 338 nm through a longpass filter. Subsequently, the solution in the cuvette was diluted twofold, in order to maintain the peptide concentration constant, and throughout the titration the emission spectra and total fluorescence intensities were recorded. The dilution was performed until the critical micelle concentration of each surfactant was reached. The observed polarization (P) was related to the fraction of peptide bound (x) with the equation: [9]

$$x = \frac{(3 - P_b)(P - P_f)}{(3 - P)(P_b - P_f) + (g - 1)(3 - P_f)(P_b - P)} \quad (3)$$

where P_b and P_f are the bound and free polarization, and g is the quantum yield enhancement factor.

2.7. Time-resolved fluorescence measurements

The lifetimes and dynamic polarizations (time-decay anisotropy) of the DGAT1 peptides were determined using frequency domain time-resolved fluorescence performed on an ISS Chronos fluorometer (ISS Inc., Champaign, IL) using a 300 nm LED for excitation (passed through a 295 nm (+/ − 10 nm) interference filter (Semrock)) and p-terphenyl (Sigma-Aldrich) dissolved in ethanol of HPLC/spectrophotometric grade (Sigma-Aldrich) as a reference (lifetime of 1.04 ns).

The phase shifts and the relative modulations of the emitted light were monitored at 20 light modulation frequencies from 30 to 200 MHz, at 25 °C (controlled with a circulating water-bath), monitoring emissions at wavelengths longer than 338 nm through a longpass filter and magic angle polarizers with the peptide Sit1 (8 μM) in PBS and in the presence of micelles of HPS and CTAB at peptide to lipid molar ratios of 1:1600, 1:800, 1:400, 1:200, 1:100, and 1:50. Lifetime data were analyzed using discrete, Lorentzian and Gaussian distribution models, judging the goodness of fit of the measured phase and modulation data by the value of the reduced χ^2 [11]. In addition, the phasor approach [9, 12, 13] was employed to examine the complex decay of the peptides upon lipid binding. The phasor approach has been described in detail elsewhere, but briefly, using either frequency domain or time domain data, a phasor plot may be constructed which provides a simple geometrical representation of the time-resolved data. The basic concept for frequency domain data is as follows. Given phase (Φ) and modulation (M) values at a particular light modulation frequency, two values, termed S and G, can be calculated by the expressions: $G = M\cos\Phi$ and $S = M\sin\Phi$ (These parameters were first described by Gregorio Weber [14]). Using these G and S values, one can construct a plot as shown in figure 2(c). These types of plots have been called phasor plots [12], polar plots [15] and AB plots [16–18]. The perimeter of this curve is known as the 'universal circle', and all single exponential lifetimes must fall somewhere on this circle. Multiple exponential decays will give rise to points inside this universal circle [9]. Phasor diagrams have been used to investigate both the intensity decay and the time-decay anisotropy of proteins and other fluorophores [13, 16, 19–23].

Dynamic polarization measurements [11] were performed with excitation at 300 nm with the peptides in aqueous solution, 50% glycerol and in the presence of the micelles at 1:1600 peptide to lipid molar ratio. Emission was monitored at wavelengths longer than 338 nm using a longpass filter for the vertically and horizontally polarized components of fluorescence intensity, at 20 frequencies from 20 to 250 MHz.

Table 1. Rotational correlation coefficients of the DGAT1 peptides in aqueous solution.

Sample	θ_1	θ_2	x_1	x_2	χ^2
PBS (pH 7.2), 25 °C					
Sit1	1.83	0.15	0.035	0.26	0.984
Sit2	1.21	0.079	0.068	0.28	0.509
Sit1 and 2	1.60	0.068	0.075	0.22	0.624
average	1.54	0.98	0.059	0.25	
50% glycerol, 25°C					
Sit1	3.06	0.114	0.116	0.18	0.447
Sit2	3.44	0.112	0.129	0.22	0.651
Sit1 and 2	3.89	0.106	0.125	0.18	0.384
average	3.46	0.110	0.123	0.19	

r_0 values were determined for Sit1 (0.30), sit2 (0.35), and Sit1 and 2 (0.30) in 100% glycerol, at 5 °C with excitation at 300 nm.

2.8. Effects of temperature and quencher on the lifetime

The excited state decay of the peptide Sit1 in aqueous solution and in the presence of HPS micelles (10 mM) was examined as a function of temperature ranging from 20 to 45 °C (controlled with a circulating water-bath) in 5 °C steps, allowing 10 min incubation at each point. In addition, the effect of 0 − 0.1 M acrylamide at 25 °C on the excited state decay of Sit1 in aqueous solution and in the presence of the HPS micelles was investigated. Lifetime analysis using discrete models, Lorentzian distribution and the phasor approach were performed to elucidate the effects of temperature and quencher.

3. Results and discussion

3.1. Peptides in aqueous solution

The quantum yield of Trp residues in folded proteins has been found to vary from near zero to 0.35 [24, 25]. The relative fluorescence quantum yield of the DGAT1 peptides in aqueous solution at 25 °C was determined to vary from 0.05 to 0.14 (Supplementary table 1 (stacks.iop.org/MAF/3/025003)). Previous work with the DGAT1 peptides (Sit1, Sit2 and Sit1 and 2) has demonstrated their disordered structure in aqueous solution [8]. In agreement with the lack of regular structure of the peptides, their corrected emission spectra in PBS (figure 1(a)) presented emission maximum centered at 355 nm, suggesting that the Trp residues in each peptide are in a polar environment (likely exposed to the aqueous environment).

The low polarization values (~0.05) observed in the excitation polarization spectra (below 300 nm) of the peptides in PBS (figure 1(b)) indicated the fast rotation of the Trp residues, due to their high local mobility, which was similar to that expected for the free fluorophore in solution, or when it is located within a very flexible/unfolded region of a polypeptide. These results correlated well with previous data [8].

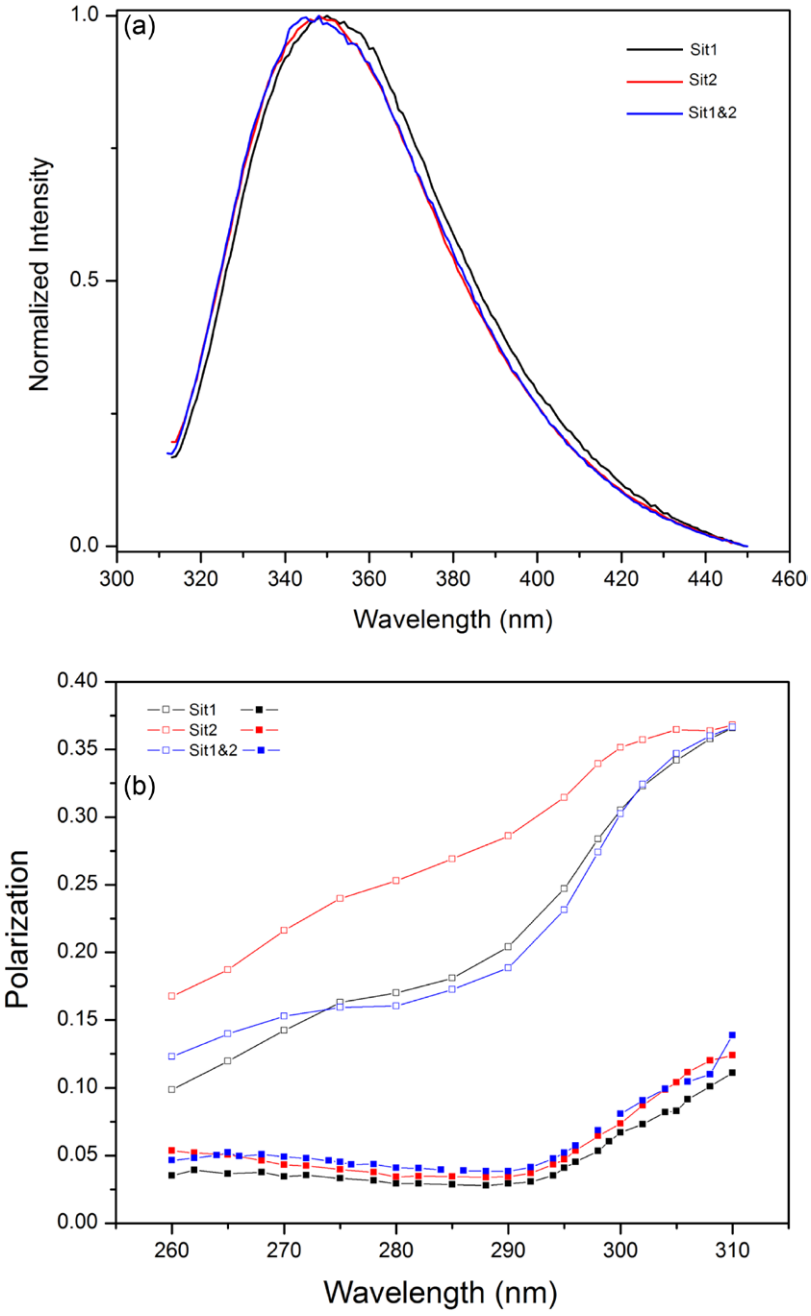

Figure 1. (*a*) Corrected parallel polarized emission spectra of the peptides Sit1 (black), Sit2 (red), and Sit1 and 2 (blue) in PBS, pH 7.2 and (*b*) excitation polarization spectrum of the peptides in PBS at 25 °C (closed squares) and in 100% glycerol at 5 °C (open squares).

Increasing the viscosity of the solution with 50% glycerol (data not shown), increased the polarization values and resulted in an increase in all polarization values of the DGAT1 peptides. The shifts were due to the reduction of the rotation diffusion of the Trp residues in this solvent. Moreover, when the solvent viscosity was increased further (with 100% glycerol) and when peptides were incubated at low temperature (5 °C), the polarization values were even higher (figure 1(*b*)), suggesting a significant reduction of the fluorophore mobility in this condition, due to the reduction of the peptide rotation.

Interestingly, in this environment of low temperature and higher viscosity, it was possible to observe an additional depolarization, i.e. beyond that expected by rotational diffusion, of the fluorescence at the region from 260 to 300 nm in Sit1 and Sit1 and 2. Given that Sit1 and Sit1 and 2 contain 2 and 3 Trp residues, respectively, while Sit 2, has only one tryptophan, it is likely that the additional depolarization in this region occurred via transfer of the excited state energy between the Trp residues (homo-transfer) in peptides containing more than one tryptophan residue. In addition, when the excitation was performed near the red-edge of the absorption band of the Trp (>300 nm), the polarization curves of the three peptides converged. This lack of homoenergy transfer upon excitation near the red-edge of the absorption band of Trp is a phenomenon known as the Weber red-edge effect [26, 27].

The excited state lifetimes of the Trp in the DGAT1 peptides were measured with time-resolved fluorescence using the frequency domain method. Figure 2(*a*) is a frequency-response curve that shows on *x*-axis the range of frequencies (from 20 to 250 MHz) used for excitation of Sit2 in aqueous solution, the respective phase delay of the emission measured on each point (on left-*y*-axis), and the ratio between the modulation of the emitted light to that of the exciting light (on right *y*-axis). Using the phase delay and the modulation ratio one can determine a phase lifetime (τ_p) and a modulation lifetime (τ_M), when both are equal at all modulation frequencies, the fluorescence decay is single exponential. The decay of the intensity of the peptides in aqueous solution could not be well-fitted by a single exponential model, and two or three discrete exponentials were used for analyzing their decay. For Sit2 (figure 2(*a*)), the decay times which fitted best were 3.3, 1.3 and 0.14 ns, with fractional intensities of 54, 36 and 10%, respectively. The lifetime heterogeneity determined for the single-Trp peptide at neutral pH, as observed in Sit2, is a common feature of single-tryptophan containing proteins and peptides [24, 28]. An alternative approach to analyze the lifetime of tryptophan residues based on protein dynamics was proposed in terms of multiple interconverting conformations [29], in which a continuous distribution of decay times can result from the interconversion between the Trp conformations. The physical basis for the distributions resides in the interconversion between conformations, each characterized by a quasi-continuum of energy substates, which place the tryptophan residue in different environments. The observed lifetime heterogeneity, according to this line of reasoning, is thus a function of the interconversion rates and hence the assignment of a discrete lifetime component to a particular protein conformation may be an over simplification. For Sit1 and Sit1 and 2, the presence of multiple Trp of course adds to the complexity of the intensity decay.

The fluorescence lifetimes of the Trp emission in each peptide were higher in 50% glycerol than in PBS. The decay of the Trp emission in Sit2 (figure 2(*a*)), for instance, could be fitted with three exponentials of 5.7, 2.3 and 0.38 ns, representing 43, 43 and 14%, contributions to the intensities, respectively. The complete analysis of the complex excited state decay of the Trp in each peptide using a discrete model are given in supplementary table 2 (stacks.iop.org/MAF/3/025003). In addition, the use of Lorentzian and Gaussian distribution models (supplementary tables 3–4 (stacks.iop.org/MAF/3/025003)) to fit the excited state decay of the peptides showed the increase of the central lifetimes and the broadening of the distribution when viscosity was increased.

Analysis of the dynamic polarization (time-decay anisotropy) of the peptides in aqueous solution revealed a multiexponential behavior, due to the presence of multiple rotational modes of their Trp residues, which can be seen as a mixed global and localized diffusion of the fluorophore. All three peptides presented two fast rotational correlation times (table 1), with averages of 1.54 ns and 98 ps. The dynamic polarization of Sit2 in PBS (figure 2(*b*)) shows a continuous increase of the delta phase values with the increase of modulation frequency, in agreement with the fast correlation times (1.21 ns and 79 ps) for this peptide. The longer rotational correlation time is attributed to the rotation of the entire molecule (global motion) in the solution, while the more rapid component may be attributed to the internal rotation involving Trp (local motion). These two values are in good correlation with the dynamic polarization of the Trp residue in the antimicrobial peptide mellitin [30], which is an unstructured monomeric 26-residue peptide in solution, where two rotational modes were observed, one with a rotational correlation time of about 160 ps and the other of 1.7 ns. The curve of dynamic polarization for the peptides in the presence of 50% glycerol was clearly altered from that in PBS (figure 2(*b*)), suggesting the reduction of the rotational diffusion of the fluorophore, due to an increase in the longer rotational correlation time to 3.46 ns.

Analysis of tryptophan fluorescence decay itself is not trivial and the presence of multiple Trp residues in a protein/peptide complicates this analysis. This heterogeneity of single tryptophan proteins has been attributed to emission from different rotamers of the indole rings. However, it is now known that the lifetime of tryptophan in proteins is affected by many processes, which enhance the non-radiative decay rate, including solvent quenching, excited state proton transfer, excited state electron transfer, intersystem crossing, and quenching by excited state proton or electron transfer by several amino acid residues as well as peptide bonds [11]. Disulfide bonds have also been implicated in tryptophan quenching. Hence, analysis of the lifetime data multiple discrete components or in terms of distribution models is not straightforward. The phasor method provides an alternative graphical way to facilitate the investigation of such complex systems and to provide a model-free approach where data fitting is not required to investigate the effects of various conditions on the intensity decay [13, 19, 21, 23, 31].

Phasor diagrams were thus employed to view the fluorescence intensity decay of the DGAT1 peptides in aqueous solution. For each peptide, all the phasor points obtained using different modulation frequencies were within the universal circle, indicating that their intensity decays are not single exponentials. In addition, the points on the phasor plot for Sit2 in the presence of glycerol (figure 2(*c*)) showed a counterclockwise movement compared to the points at the same frequencies in PBS, reflecting that the higher the viscosity, the higher the average excited state lifetimes of the peptides.

In a similar way, the phasor treatment of the dynamic polarization of Sit2 (figure 2(*d*)), changed to a more pronounced curved, that can be interpreted as the reduction of the rotational mobility of the Trp residues, or the dominance of one of the rotational modes over

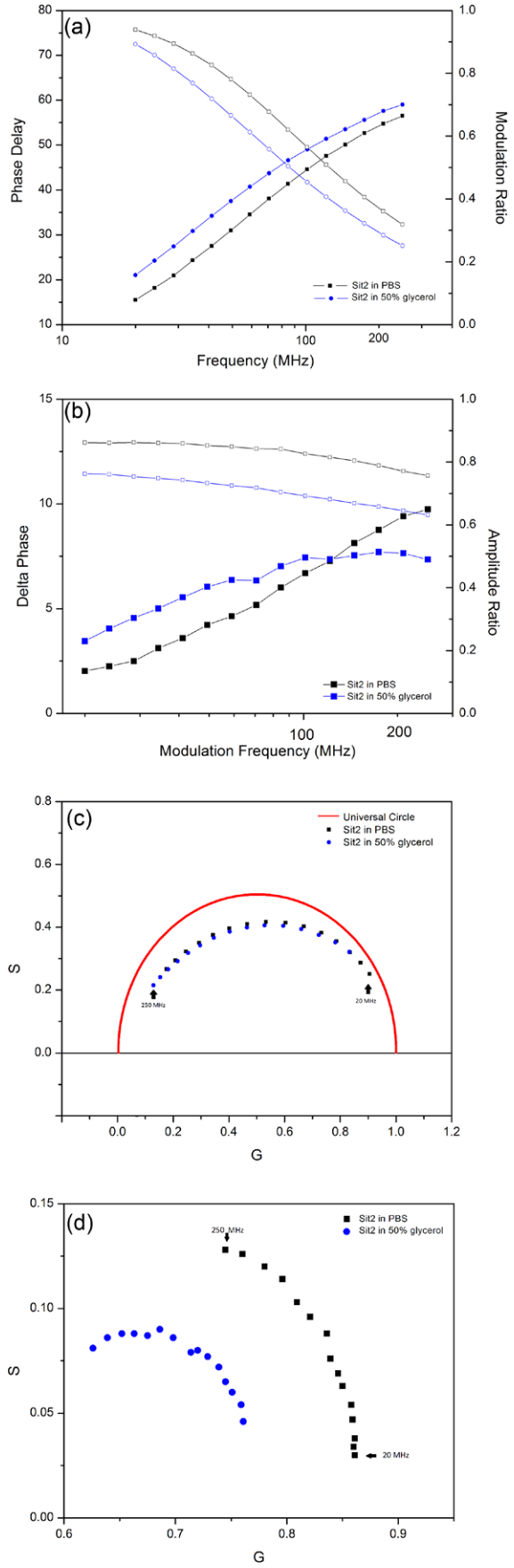

Figure 2. Frequency domain time-resolved fluorescence measurements of (*a*) intensity decay and (*b*) dynamic polarization of Sit2 in PBS (black) and in 50% glycerol (blue). Variation of phase (closed symbols) and modulation (open symbols) of Trp residue were monitored as a function of frequency (from 20 to 250 MHz); Phasor plots of the (*c*) intensity decay and (*d*) dynamic polarization of Sit2 in PBS (black) and in 50% glycerol (blue).

the other [23]. Similar behaviors were observed for the fluorescence intensity decay and dynamic polarization of the peptides Sit1 and Sit1 and 2 in PBS/glycerol on the phasor diagram (supplementary figure 1 (stacks.iop.org/MAF/3/025003)).

3.2. Peptides in the presence of membrane models

The interaction of the DGAT1 peptides with zwitterionic, negatively charged or positively charged surfactants resulted in blue shifts of the fluorescence emission maxima (supplementary figure 2 (stacks.iop.org/MAF/3/025003)). In order to better investigate the different binding of the peptides in this membrane model other fluorescence properties were investigated. The excitation polarization spectra of the peptides in the presence of the detergents (supplementary figure 2 (stacks.iop.org/MAF/3/025003)), indicate the binding of Sit1 in all types of surfactants, as evidenced by the reduction in the mobility of its Trp residues in the three models used. With the other two peptides (Sit2 and Sit1 and 2), the increase of polarization was more evident in the surfactant with the negatively charged head group, suggesting that an electrostatic attraction between these peptides with negatively charged surfaces can modulate their interaction, in agreement with previous data [8], which describe the binding of Sit1 to the acyl-CoA molecule via the acyl chain of the substrate, while the binding of Sit 2 to membranes can be modulated by the presence of negatively-charged domains at the surface.

Solute fluorescence quenching in model membranes is often controlled by the degree to which small solute quenchers (like acrylamide) are partitioned into the hydrocarbon-like subphases of these structures, and by the diffusion coefficient of the quencher within the subphases [32]. The Stern–Volmer quenching constants for acrylamide (table 2) determined for the peptides in aqueous solution were higher (average of 9.7 M^{-1}) than in the presence of the model membranes, reflecting that binding to the micelle has reduced the exposure of the Trp residues to the quencher, probably due to the access of the Trp within the acyl core of the micelles or at the lipid-water interface. Sit1 and Sit1 and 2 showed a very similar behavior (supplementary figure 3 (stacks.iop.org/MAF/3/025003)), with a partial insertion on the zwitterionic and positively-charged micelle, and a deeper insertion when interacting with the negatively charged surfactant. The access of the quencher to the Trp-residue of Sit2 is not altered in the presence of the positively charged micelle, which was the only condition in which the same quenching constant for the peptide in aqueous solution was found. However, in the presence of the negatively charged surfactant, Sit2 presented the lowest K_{SV} value (3.5 M^{-1}); suggesting the deepest insertion of the Trp occurred in this model membrane.

When bound to the membrane models, the excited state lifetime of the peptides could be described in terms of only two exponential terms (supplementary figure 4 (stacks.iop.org/MAF/3/025003)), whose components were increased over those of the free peptide, assuming average values of 5.4 and 1.5 ns, suggesting that the local environment of the Trp residues changes upon binding to the model membrane. Figure 3(*a*) shows the increase of the excited state decay of Sit2 in the presence of the zwitterionic micelle. The reduction of the number of lifetime components when a Trp-containing peptide is bound to a membrane model has previously been suggested to be due to the reduction of the number of rotamer forms of the Trp residues in the peptide. Similar fluorescence decays were found in a series of single-Trp containing peptides when forming peptide-lipid complexes [33], in which only two exponential terms of average values of 6.9 and 2.7 ns with fractional amplitudes of 30 and 70%, respectively, were required for good fits upon binding to the membrane model. In addition, the dynamic polarization curves of the peptides bound to the micelles (figure 3(*c*)) revealed the reduction of the rotational modes of the Trp residues, due to the decreased mobility of the peptides in the peptide-lipid complexes.

Phasor plots of the excited state decay (figure 3(*b*)), and dynamic polarization (figure 3(*d*)), of the peptides bound to the lipid systems showed a behavior similar to that observed in the solution of high viscosity, in which a counterclockwise shift of the points within the universal circle and a more closed curve were observed, respectively. The movement of the points on the phasor diagram revealed that the mobility of the Trp residues was clearly reduced upon binding to the micelles.

The relative quantum yield of the peptides (supplementary table 1 (stacks.iop.org/MAF/3/025003)) increased by about 5-fold in the presence of the zwitterionic (HPS) or cationic (CTAB) micelles, but it was reduced by about 4-fold upon binding to the negatively charged surfactant (SDS). As the quantum yield of the peptides was significantly altered upon interaction with the model membranes, a quantum yield enhancement factor was considered to correct the expressions relating the fluorescence parameters [9]. Steady-state fluorescence methods were applied to monitor the binding of the Sit1 peptide in the micelles in terms of the movement of the spectral center of mass (figure 4(*a*)), polarization (figure 4(*b*)) and total intensity changes upon binding to the lipids. The binding curve was fitted and an average $K_d \sim 1$ mM was found. Individual values are in supplementary table 5 (stacks.iop.org/MAF/3/025003).

Table 2. Acrylamide quenching constants (K_{SV}) of the DGAT peptides free and bound to the model membranes.

	Sit1	Sit2	Sit1 and 2
	K_{SV} (M^{-1})	K_{SV} (M^{-1})	K_{SV} (M^{-1})
PBS (pH 7.4)	9.1	9.1	11
10 mM SDS	4.8	3.5	4.1
10 mM HPS	7.6	7.7	8.0
10 mM CTAB	7.7	9.5	7.7

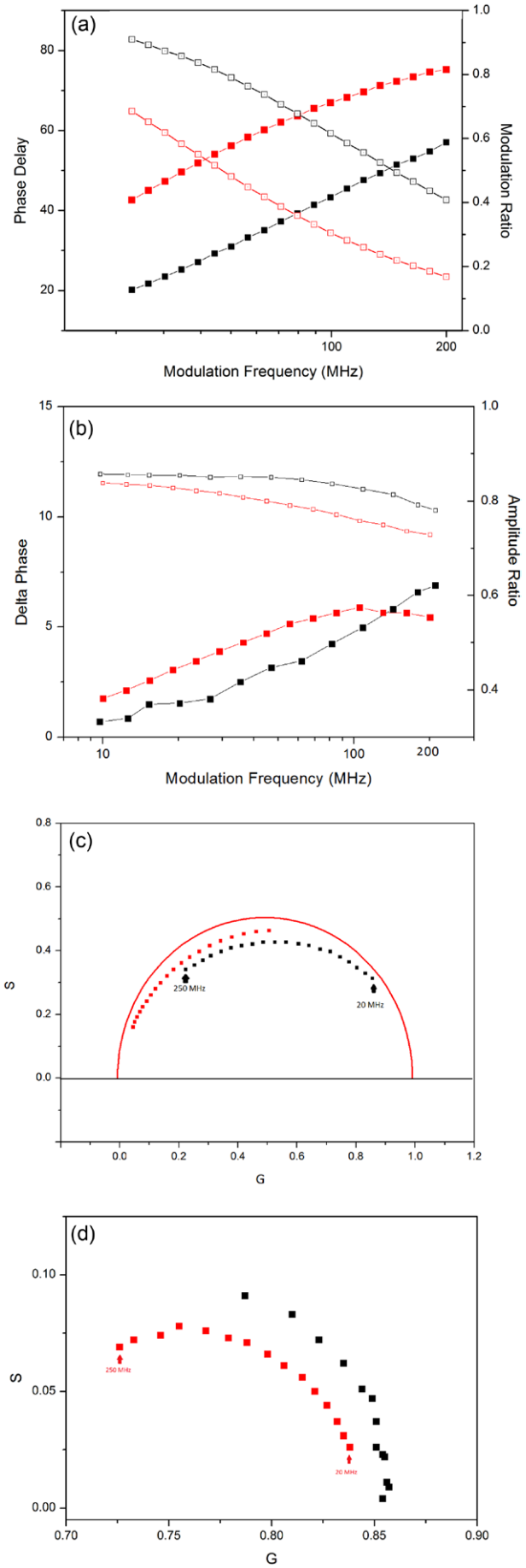

Figure 3. (*a*) Phase delay (closed symbols) and modulation ratio (open symbols) of the excited state lifetime of Sit1 in aqueous solution (black) and in the presence of micelles of HPS (red) and (*b*) dynamic polarization of the peptides Sit1 in the presence of the zwitterionic micelles (red) and (*c* and *d*) their respective phasor diagrams.

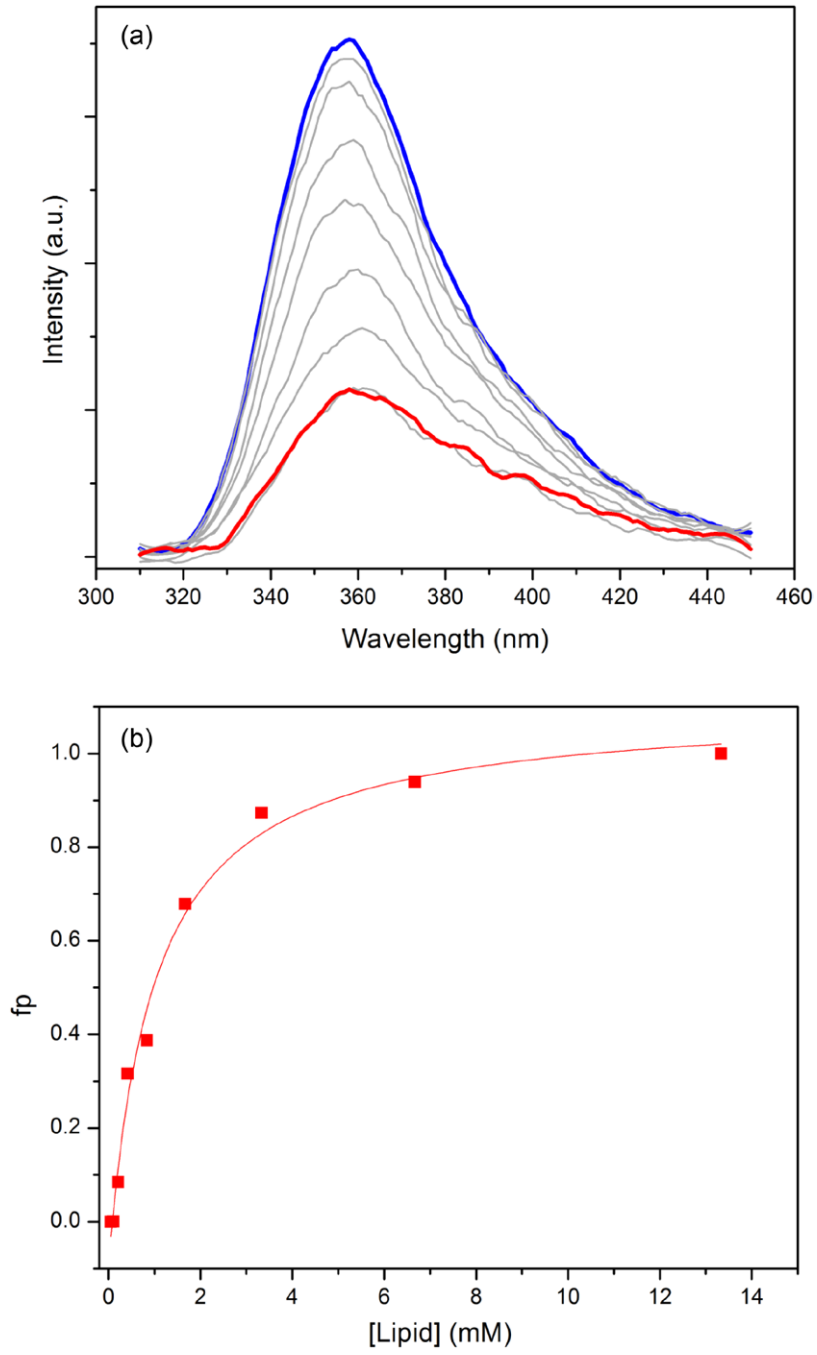

Figure 4. Effect of the lipid binding on the (*a*) emission spectra and (*b*) anisotropy of the Trp residues of Sit1 in zwitterionic micelles used in the range of 1:100 (red) to 1:1600 peptide (blue) to lipid molar ratio. Intermediate peptide to lipid molar ratio is in gray.

3.3. Phasor analysis of peptide-lipid complexes

Phase/modulation studies were performed as a function of temperature, from 20 to 45 °C, with Sit1 in PBS and in the presence of the HPS micelles (supplementary figure 5(*a*)) (stacks.iop.org/MAF/3/025003). These data were analyzed with a Lorentzian distribution fit (supplementary table 6 (stacks.iop.org/MAF/3/025003)), which showed a gradual decrease of the central values of the distribution (from 1.9 to 1.1 ns) as the temperature was increased, i.e. faster excited state decays of Sit1 were obtained at elevated temperatures, and in addition, the full-width half-maximum of the distributions were also reduced (from 1.6 to 0.7 ns) as a consequence of the temperature elevation (supplementary figure 5(*c*) (stacks.iop.org/MAF/3/025003)). This decrease in the width of the distribution as a function of temperature elevation is in agreement with the observations described for single-Trp proteins [28, 34]. The Arrhenius plot of the fluorescence lifetime data (supplementary figure 5(*d*) (stacks.iop.org/MAF/3/025003)) was performed with the central lifetime of the Lorentzian distribution fits, and gave Arrhenius activation energy (*Ea*) of ~1.9 kcal mol^{-1} for the peptide in aqueous solution and 1.37 kcal mol^{-1} for the peptide bound to the micelles.

The phasor diagram of these data (supplementary figure 5(*b*) (stacks.iop.org/MAF/3/025003)) for points at different temperature but the same light modulation frequency (100 MHz) shows that the higher the

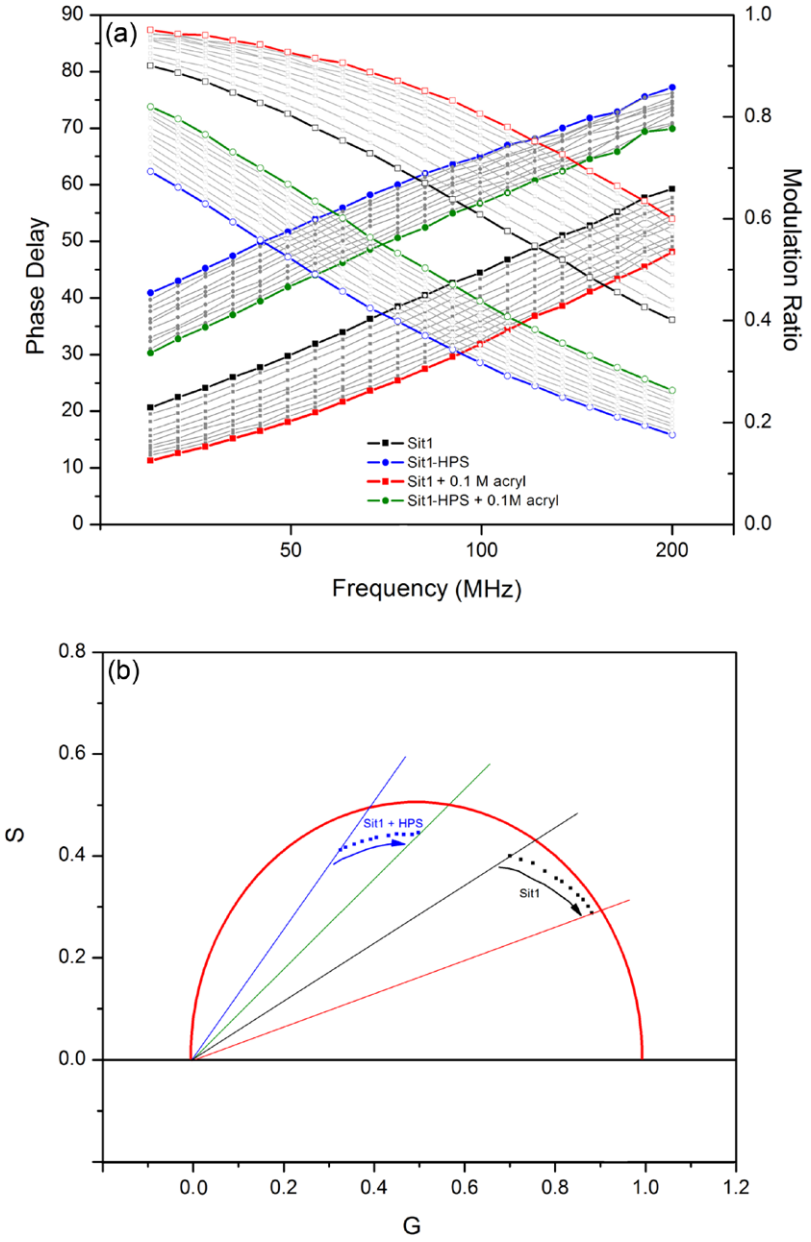

Figure 5. (*a*) Phase delay (closed symbols) and modulation ratio (open symbols) of the excited state lifetime of Sit1 in aqueous solution (black) and in the presence of micelles of HPS (blue) throughout the acrylamide titration. Red and green curves correspond to the 0.1 M acrylamide in the free and lipid bound peptide, respectively. Intermediate acrylamide concentrations are in gray, and (*b*) phasor diagram for the quenching assays with Sit1 free (black) and bound to HPS (blue). Points are for modulation frequency of 50 MHz.

temperature, the shorter the lifetimes, with points presenting a trajectory that goes along the universal circle. Similar shape trajectories were observed in the absence and in the presence of the model membrane.

Frequency-domain time-resolved fluorescence data were obtained with Sit1 in the presence of the quencher acrylamide (figure 5(*a*)). A discrete model was used here, and showed that both longer and shorter components of fluorescence lifetimes of Sit1 were decreased in the presence of the quencher (supplementary table 7 (stacks.iop.org/MAF/3/025003)). The classic form of the Stern–Volmer equation (given in equation (2)) is equal to the ratio τ_0/τ, where τ_0 and τ are the lifetimes of the fluorophore in the absence and in the presence of the quencher, respectively. However, a straightforward interpretation of the Stern–Volmer relation is valid only when a simple monoexponential decay is observed, which was clearly not the case in the Trp residues of the DGAT1 peptides. A mean lifetime from the two-component analysis, weighted for their respective fractions was obtained and analyzed into a linear curve in the Stern–Volmer plots, with values of 8.4 and 4.6 M^{-1}, for the peptide in PBS and in the presence of HPS micelles, respectively (supplementary figure 6 (stacks.iop.org/MAF/3/025003)). The quenching trajectory on the phasor diagram, both in aqueous solutions and in the presence of the micelles of HPS (figure 5(*b*)), is in agreement with the reduction of the lifetime in the presence of the quencher, and show trajectories along the universal circle for the free and bound peptide.

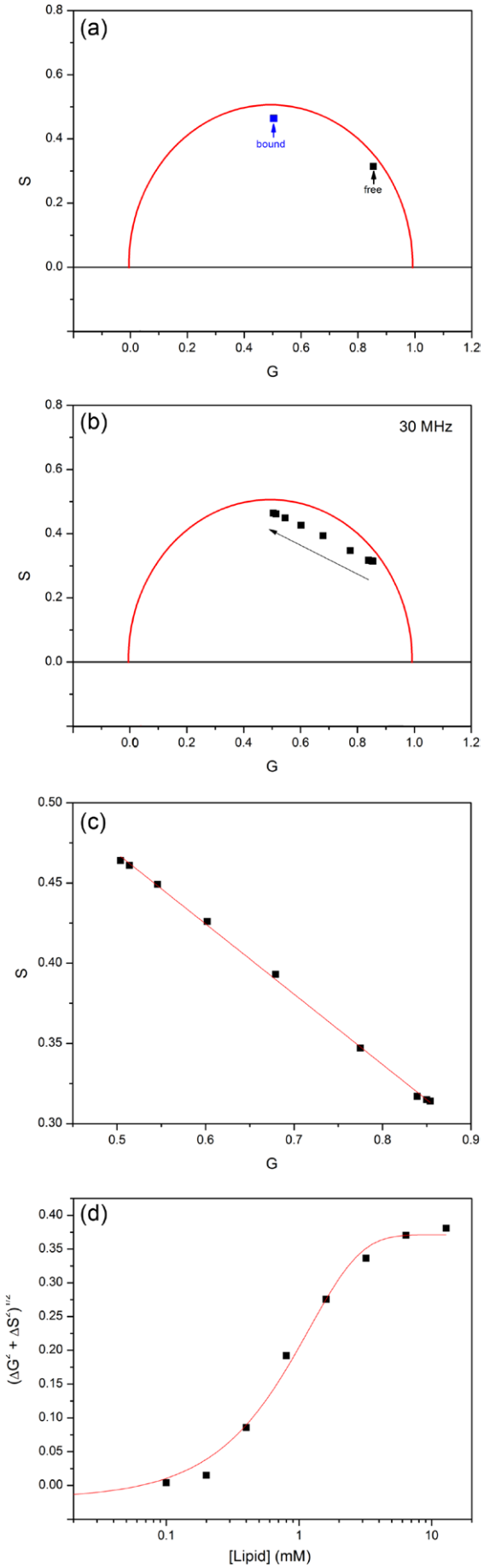

Figure 6. Phasor plots of the (*a*) free and bound state of Sit1 in the HPS micelles and (*b*) intermediate points throughout the titration. Points are for modulation frequency of 30 MHz. (*c*) Straight line connecting the points on the phasor diagram and (*d*) Bjerrum plot for titration of Sit1 in the HPS micelles.

The binding of Sit1 in the micelles of HPS was monitored by following the points on the phasor diagram of the free and bound state of the peptide (figure 6(*a*)), and throughout the titration of the zwitterionic micelle (figure 6(*b*)). Comparing the points of each single frequency (30 MHz are shown), it was possible to determine a straight line trajectory connecting the two points of the free and bound peptide (figure 6(*c*)), revealing that any points during the titration can be described by a linear combination of the two states of the peptide. Plotting the points of the titration as a function of the concentration of the lipids (figure 6(*d*)), gave K_d of the peptide to the micelles with an average of ~1 mM, which correlated well to the dissociation constants determined by steady-state approaches. The phasor plot, in addition to being a rapid and facile qualitative approach for investigating the complex decay of multifluorophores systems, like proteins, can be applied for determining quantitative parameters of the interaction of those complex systems (proteins) with their ligands (lipid systems), by monitoring the trajectory of the points in the phasor diagram. Similar treatment was employed for the binding of Sit1 in the CTAB micelles (supplementary figure 7 (stacks.iop.org/MAF/3/025003)).

4. Conclusions

Steady-state and time resolved fluorescence methods are useful techniques to study the high flexibility and the disordered state of the DGAT1 peptides in aqueous solution and are suitable approaches to monitor the conformational changes of these peptides when bound to the lipid systems, which resulted in significant reduction of the mobility of their Trp residues.

In this sense, in the system investigated here, the putative binding sites of DGAT1, which were predicted to be allocated into a large luminal extramembranous loop of the enzyme [8], exhibited interactions at the membrane surface; however, all peptides were able to access the hydrophobic core of the lipid systems, possibly for assessing their lipid substrates (acyl-CoAs and diacylglycerols). Knowledge of the dynamics of the DGAT1 peptides in different environments (especially those that mimic the membrane-bound state of the enzyme) and the factors that can affect their dynamics provide new insights related to the regulation of this important enzyme, which may be useful in the design of compounds which can modulate the activity of DGAT1.

Acknowledgments

The authors thank the Sao Paulo Research Foundation (FAPESP) for the grants 2009/17698-5, 2010/13036-5 and 2013/20414-4 (to JLSL).

References

[1] Yen C L E, Stone S J, Koliwad S, Harris C and Farese R V Jr 2008 DGAT enzymes and triacylglycerol biosynthesis *J. Lipid Res.* **49** 2283–301

[2] Coleman R A and Lee D P 2001 Enzymes of triacylglycerol synthesis and their regulation *Prog. Lipid Res.* **43** 134–76

[3] Liu Q, Siloto R M, Lehner R, Stone S J and Weselake R J 2012 Acyl-CoA:diacylglycerol acyltransferase: molecular biology, biochemistry and biotechnology *Prog. Lipid Res.* **51** 350–77

[4] Birch A M, Buckett L K and Turnbull A V 2010 DGAT1 inhibitors as anti-obesity and anti-diabetic agents *Curr. Opin. Drug Discovery Dev.* **13** 489–96

[5] DeVita R J and Pinto S 2013 Current status of the research and development of diacylglycerol O-acyltransferase 1 (DGAT1) inhibitors *J. Med. Chem.* **56** 9820–5

[6] Cao J *et al* 2011 Targeting Acyl-CoA: diacylglycerol acyltransferase 1 (DGAT1) with small molecule inhibitors for the treatment of metabolic diseases *J. Biol. Chem.* **268** 41838–51

[7] Zammit V A, Buckett L K, Turnbull A V, Wure H and Proven A 2008 Diacylglycerol acyltransferases: potential roles as pharmacological targets *Pharmacol. Ther.* **118** 295–302

[8] Lopes J L S, Nobre T M, Cilli E M, Beltramini L M, Araújo A P U and Wallace B A 2014 Deconstructing the DGAT1 enzyme: binding sites and substrate interactions *Biochim. Biophys. Acta* **1838** 3145–52

[9] Jameson D M 2014 *Introduction to Fluorescence* (New York: CRC Press)

[10] Chen R F 1967 Fluorescence quantum yields of tryptophan and tyrosine *Anal. Lett.* **1** 35–42

[11] Ross J A and Jameson D M 2008 Time-resolved methods in biophysics 8. Frequency domain fluorometry: applications to intrinsic protein fluorescence *Photochem. Photobiol. Sci.* **7** 1301–12

[12] Jameson D M, Gratton E and Hall R D 1984 The measurement and analysis of heterogeneous emissions by multifrequency phase and modulation fluorometry *Appl. Spectrosc. Rev.* **20** 55–106

[13] Stefl M, James N G, Ross J A and Jameson D M 2011 Applications of phasors to *in vitro* time-resolved fluorescence measurements *Anal. Biochem.* **410** 62–9

[14] Weber G 1981 Resolution of the fluorescence lifetimes in a heterogeneous system by phase and modulation measurements *J. Phys. Chem.* **85** 949–53

[15] Redford G I and Clegg R M 2005 Polar plot representation for frequency-domain analysis of fluorescence lifetimes *J. Fluoresc.* **15** 805–15

[16] Hanley Q S and Clayton A H 2005 AB-plot assisted determination of fluorophore mixtures in a fluorescence lifetime microscope using spectra or quenchers *J. Microsc.* **218** 62–7

[17] Clayton A H 2008 The polarized AB plot for the frequency-domain analysis and representation of fluorophore rotation and resonance energy homotransfer *J. Microsc.* **232** 306–12

[18] Clayton A H A, Hanley Q S and Verveer P J 2004 Graphical representation and multicomponent analysis of single-frequency fluorescence lifetime imaging microscopy data *J. Microsc.* **213** 1–5

[19] James N G, Ross J A, Stefl M and Jameson D M 2011 Applications of phasor plots to *in vitro* protein studies *Anal. Biochem.* **410** 70–6

[20] Bader A N, Visser N V, van Amerongen H and Visser A J W G 2014 Phasor approaches simplify the analysis of tryptophan fluorescence data in protein denaturation studies *Methods Appl. Fluoresc.* **2** 045001 (at press)

[21] Montecinos-Franjola F, James N G, Concha-Marambio L, Brunet J E, Lagos R, Monasterio O and Jameson D M 2014 Single tryptophan mutants of FtsZ: nucleotide binding/exchange and conformational transitions *Biochim. Biophys. Acta* **1844** 1193–200

[22] Fereidouni F, Blab G A and Gerritsen H C 2014 Phasor based analysis of FRET images recorded using spectrally resolved lifetime imaging *Methods Appl. Fluoresc.* **2** 035001

[23] Vetromile C M and Jameson D M 2013 Applications of phasor plots to dynamic polarization studies *Biophys. J.* **104** 682a

[24] Beechem J M and Brand L 1985 Time-resolved fluorescence of proteins *Annu. Rev. Biochem.* **54** 43–71

[25] Alston R W, Lasagna M, Grimsley G R, Scholtz J M, Reinhart G D and Pace C N 2008 Peptide sequence and conformation strongly influence tryptophan fluorescence *Biophys. J.* **94** 2280–7
[26] Weber G 1960 Fluorescence-polarization spectrum and electronic-energy transfer in tyrosine, tryptophan and related compounds *Biochem. J.* **75** 335–45
[27] Moens P D, Helms M K and Jameson D M 2004 Detection of tryptophan to tryptophan energy transfer in proteins *Protein J.* **23** 79–83
[28] Eftink M R and Wasylewski Z 1989 Fluorescence lifetime and solute quenching studies with the single tryptophan containing protein parvalbumin from codfish *Am. Chem. Soc.* **28** 382–91
[29] Alcala J R, Gratton E P and Rendergast F G 1987 Fluorescence lifetime distributions in proteins *Biophys. J.* **51** 597–604
[30] Lakowicz J R, Cherek H, Gryczynnski I, Joshi N and Johnson M L 1987 Enhanced resolution of fluorescence anisotropy decays by simultaneous analysis of progressively quenched samples. Applications to anisotropic rotations and to protein dynamics *Biophys. J.* **51** 755–68
[31] Reinhart G D, Marzola P, Jameson D M and Gratton E 1991 A method for on-line background subtraction in frequency domain fluorometry *J. Fluoresc.* **1** 153–62
[32] Eftink M R and Ghiron C A 1976 Fluorescence quenching of indole and model micelle systems *J. Phys. Chem.* **805** 486–93
[33] Clayton A H A and Sawyer W H 1999 Tryptophan rotamer distributions in amphipathic peptides at a lipid surface *Biophys. J.* **76** 3235–42
[34] Alcala J R, Gratton E and Prendergast F G 1987 Interpretation of fluorescence decays in proteins using continuous lifetime distributions *Biophys. J.* **51** 925–36